

## Discovery of Tirasemtiv, the First Direct Fast Skeletal Muscle Troponin Activator

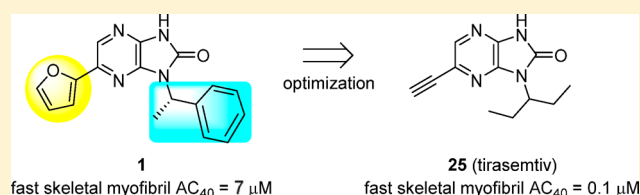
Scott E. Collibee,<sup>\*ID</sup> Gustave Bergnes, Alexander Muci, William F. Browne, IV,<sup>||</sup> Marc Garard, Aaron C. Hinken,<sup>†</sup> Alan J. Russell,<sup>‡</sup> Ion Suehiro, James Hartman, Raja Kawas, Pu-Ping Lu, Kenneth H. Lee, David Marquez, Matthew Tomlinson,<sup>⊥</sup> Donghong Xu, Adam Kennedy, Darren Hwee, Julia Schaletzky, Kwan Leung, Fady I. Malik, David J. Morgans, Jr.,<sup>§</sup> and Bradley P. Morgan

Cytokinetics, Inc., 280 East Grand Avenue, South San Francisco, California 94080, United States

### S Supporting Information

**ABSTRACT:** The identification and optimization of the first activators of fast skeletal muscle are reported. Compound **1** was identified from high-throughput screening (HTS) and subsequently found to improve muscle function via interaction with the troponin complex. Optimization of **1** for potency, metabolic stability, and physical properties led to the discovery of tirasemtiv (**25**), which has been extensively characterized in clinical trials for the treatment of amyotrophic lateral sclerosis.

**KEYWORDS:** Amyotrophic lateral sclerosis (ALS), skeletal muscle activator, troponin, tirasemtiv, imidazo[4,5-*b*]pyrazin-2-one



Direct activation of skeletal muscle has the potential to improve physical performance in patients with compromised muscle function, such as those suffering from amyotrophic lateral sclerosis (ALS),<sup>1</sup> spinal muscular atrophy,<sup>2</sup> and Charcot–Marie–Tooth disease.<sup>3</sup> Muscle impairment in these disease states occurs from diminished neuromuscular input and can lead to disability and increased mortality.<sup>4</sup> Current treatment options are limited or nonexistent and represent a significant unmet medical need.<sup>5–7</sup> Precedent for activation of muscle function exists with omecamtiv mecarbil, a direct cardiac muscle activator that improves contractility and is undergoing clinical trials for the treatment of heart failure.<sup>8,9</sup> This report describes the identification and optimization of the first direct activators of fast skeletal muscle, culminating in the discovery of tirasemtiv (**25**), a compound that was found to selectively sensitize the sarcomere of fast skeletal muscle to calcium and increase its force production via interaction with the regulatory troponin complex.<sup>10</sup>

Skeletal muscle is classified into two main forms, fast skeletal muscle (Type II fibers) and slow skeletal muscle (Type I), which differ in usage, metabolism, and sarcomere composition. Fast skeletal muscle fibers have unique myosin and troponin components compared to cardiac and slow skeletal muscle, while slow skeletal muscle fibers have the same myosin and troponin C (TnC, a subunit of the regulatory complex) as cardiac muscle. Myosin is the molecular motor responsible for contractility where chemical energy from adenosine triphosphate (ATP) hydrolysis is coupled to force generation. The troponin complex plays a regulatory role by acting as a calcium sensor and resides in the thin filament along with actin and tropomyosin. The sequence homology between fast and slow muscle myosin and troponins C, T, and I is about 50%, providing a good

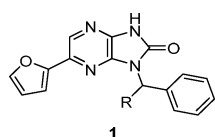
opportunity to find selective skeletal muscle troponin activators.<sup>11</sup> Because skeletal muscle is mainly responsible for voluntary movement and has unique myosin and troponin components compared to other muscle types, fast skeletal muscle represents a compelling target for small molecule intervention.

Compounds with the potential to modulate human muscle function were identified using a high-throughput screen (HTS) that measures the rate of ATP hydrolysis in rabbit fast skeletal muscle myofibrils as a surrogate for force generation in skeletal muscle.<sup>12</sup> Biochemical activity (AC<sub>40</sub>) is defined as the compound concentration that produces a 40% increase in myofibril ATPase activity at 25% of the calcium concentration needed for a maximal response in control preparations. Among the hits was imidazopyrazinone **1** (CK-1303249). Compound **1** displayed modest biochemical potency (AC<sub>40</sub> = 7.0 μM), ligand and lipophilic efficiencies (LE and LipE) of 0.32 and 5.01, respectively,<sup>13,14</sup> and specificity for fast skeletal muscle over slow skeletal, cardiac, and smooth muscle (Table 1, data not shown for smooth muscle). Additionally, **1** showed a eudismic ratio (>7) that is suggestive of a specific interaction between the molecule and a biological target (**1** vs **2** in Table 1). To determine whether activation occurs via the myosin or regulatory complex, mixed sarcomeres were created using myosin and thin filament preparations from fast, slow, and cardiac muscle sources, and each was then assayed in the presence of **1**. Because activation was observed only in combinations containing fast skeletal thin filaments, **1** was determined to be a direct troponin complex activator.<sup>10</sup>

Received: December 27, 2017

Accepted: February 13, 2018

Published: February 13, 2018

**Table 1. Activity and Selectivity of HTS Hit and Close-in Analogues<sup>a</sup>**

#	R	FSK AC <sub>40</sub> (μM)	CV AC <sub>40</sub> (μM)	SSK AC <sub>40</sub> (μM)
1	S-Me	7	>49	>39
2	R-Me	>49		
3	H	>49		

<sup>a</sup>FSK = fast skeletal muscle; CV = cardiac muscle; SSK = slow skeletal muscle.

The observed increase in ATP hydrolysis in the presence of **1** was subsequently shown using the skinned fiber assay to translate to improved force generation in a skinned, fast muscle fiber (Figure 1).<sup>15</sup> This assay is performed by mounting a muscle fiber

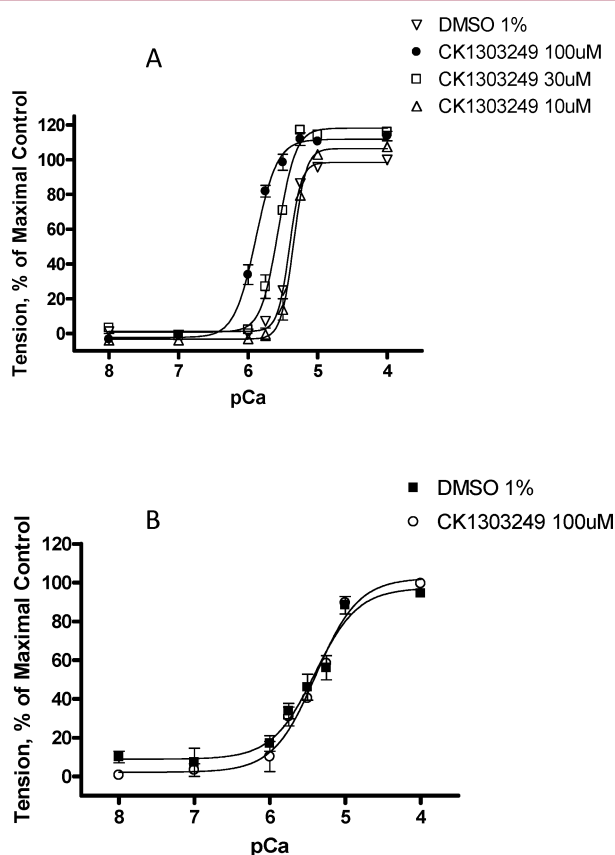


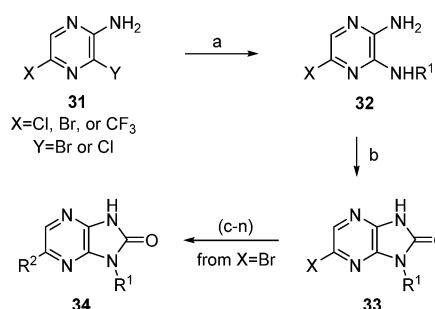
**Figure 1.** Calcium-force relationship of **1** on skinned skeletal fibers from (A) rabbit psoas muscle (fast) and (B) rabbit semimembranosus muscle (slow) plotted as % of maximal tension vs (–)log of calcium concentration (pCa).

(pretreated with detergent to remove the membranes and cytoplasm) to a force transducer rig to enable force measurement across the muscle. Treatment of primarily fast rabbit psoas muscle fibers with **1** increased the calcium sensitivity of the muscle fibers without increasing the maximum force or the shape of the curve (Figure 1A). A related control experiment using skinned, primarily slow, rabbit semimembranosus muscle fibers failed to show increased calcium sensitivity in the presence of **1** (Figure 1B). For potency comparison across compounds, DF<sub>30</sub> is

defined as the compound concentration that produces a 30% increase in tension at 25% of the calcium concentration needed for a maximal response in control preparations.

The initial optimization goals were based loosely on our previous experience with the optimization of cardiac muscle activators.<sup>9</sup> The biochemical potency needed for compounds to show physiologically significant cardiac muscle activation was between 0.1–5 μM. The desired pharmacokinetic profile would ensure that efficacious concentrations could be sustained by dosing orally once or twice per day. Therefore, the target compound profile included biochemical potency (AC<sub>40</sub>) less than 1 μM, minimal *in vitro* clearance, and good *in vivo* exposure with oral dosing.

Synthesis of the imidazo[4,5-*b*]pyrazin-2-one analogues of **1** was achieved using Scheme 1. Addition of primary amines to 2-

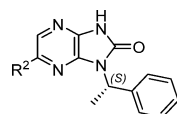
**Scheme 1. Synthesis of Imidazopyrazinone Derivatives<sup>a</sup>**

<sup>a</sup>Reagents and conditions: (a) NHR<sup>1</sup>. (b) CDI, THF. (c) (R<sup>2</sup> = furyl or phenyl) R<sup>2</sup>B(OH)<sub>3</sub>, Cl<sub>2</sub>Pd(dppf), Na<sub>2</sub>CO<sub>3</sub>, dioxane/water. (d) (R<sup>2</sup>=SMe) NaSMe, NMP. (e) (R<sup>2</sup> = OMe) NaOMe, NMP. (f) (R<sup>2</sup> = CN) Zn(CN)<sub>2</sub>, (Ph<sub>3</sub>P)<sub>4</sub>Pd, DMF. (g) (R<sup>2</sup> = Ac) tributyl(1-ethoxyvinyl)tin, Cl<sub>2</sub>Pd(dppf), dioxane. (h) (R<sup>2</sup> = H) H<sub>2</sub>, Pd/C, EtOH. (i) (R<sup>2</sup> = Me) trimethylboroxine, Cl<sub>2</sub>Pd(dppf), Na<sub>2</sub>CO<sub>3</sub>, dioxane/water. (j) (R<sup>2</sup> = H<sub>3</sub>CC≡C) H<sub>3</sub>CC≡CH, Cl<sub>2</sub>Pd(dppf), CuI, TEA, dioxane/water. (k) (R<sup>2</sup> = HC≡C). (l) 1. TMSC≡CH, Cl<sub>2</sub>Pd(dppf), CuI, TEA, dioxane/water; 2. KF, MeOH/THF/water. (m) (R<sup>2</sup> = vinyl) trimethylboroxine, Cl<sub>2</sub>Pd(dppf), Na<sub>2</sub>CO<sub>3</sub>, dioxane/water. (n) (R<sup>2</sup> = Et) from R<sup>2</sup> = vinyl; H<sub>2</sub>, Pd/C, EtOH.

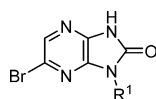
amino-3,5-halopyrazine (**31**) gave diaminopyrazines **32** in good yields, followed by ring closure using carbonyl diimidazole (CDI) to afford imidazo[4,5-*b*]pyrazin-2-ones **33**. The targeted analogues were produced in one or two steps from **34**.<sup>16</sup>

Having established calcium sensitization in isolated muscle fibers, we were interested in demonstrating improved functional activity in an animal model. We initially focused on replacing the furan in **1** to improve the metabolic stability and physical properties while exploring the structure–activity relationship (SAR) at that position. Overall, the tolerance for substitution at R<sup>2</sup> was found to be somewhat limited (Table 2). The observed potency improvement with vinyl (**5**) but not phenyl (**4**) illustrated the limited space in that region and hinted at the potential for more potent, lower molecular weight structures. The combination of reduced potency with ethyl **6** and methoxy **7**, but improved potency with SMe **8** and bromo **9**, suggesting a preference for polarizable electron-rich groups. In contrast, analogues with greater polarity (**10–12**) were much less active, pointing to intolerance for certain polar interactions at this position.

The SAR around the N1-position (R<sup>1</sup>) was examined in the context of a bromine substituent at the 6-position (Table 3). The focus was on defining a minimum pharmacophore at this

Table 2. Assessment of R<sub>2</sub>, N-1 Methylbenzyl Analogues

#	R <sup>2</sup>	AC <sub>40</sub> (μM)	DF <sub>30</sub> (μM)
1	2-furyl	7.0	30.6
4	Ph	>49	NT
5	CH=CH <sub>2</sub>	3.5	4.6
6	CH <sub>2</sub> CH <sub>3</sub>	21.8	NT
7	OMe	8.9	NT
8	SMe	2.6	3.8
9	Br	1.6	3.0
10	SO <sub>2</sub> Me	>49	NT
11	CN	>49	NT
12	COMe	>49	NT

Table 3. Assessment of N-1 position (R<sup>1</sup>)

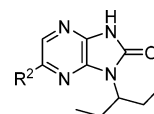
#	R <sup>1</sup>	AC <sub>40</sub> (μM)	DF <sub>30</sub> (μM)	Re (r) <sup>a</sup>	Re (h) <sup>a</sup>
9	(S)-Me-benzyl	1.6	3.0	0.5	<0.3
13	(S)-2-butyl	1.0	5.1	0.3	<0.2
14	3-pentyl	0.3	0.4 <sup>b</sup>	0.4	<0.2
15	<i>i</i> -Pr	6.0	2.2	NT	NT
16	<i>t</i> -butyl	0.8	4.6	0.3	0.2
17	cyclopropyl	>49	NT	NT	NT
18	cyclohexyl	10	NT	NT	NT

<sup>a</sup>Re = ratio of extraction in microsomes (r = rat, h = human).

<sup>b</sup>Compound 14 was tested multiple times in the skinned fiber assay (*n* = 10, standard deviation = 0.2).

position and reducing oxidative potential for the series (as measured from microsome clearance experiments).<sup>17</sup> Replacement of the phenyl group from the methylbenzyl substituent of 9 with an ethyl group (13) maintained potency and displayed improved stability in rat and human microsomes. A 3-pentyl group (14) provided a further 3-fold potency improvement in biochemical potency, excellent functional activity in the skinned fiber assay, eliminated stereochemistry from the molecule, and provided similar microsomal stability to 13. Isopropyl compound 15 lost significant potency compared to 14. The *t*-butyl substituent of 16 recovered much of the biochemical potency and presented a favorable microsomal profile, but the activity in skinned fibers was higher than expected based on its biochemical potency. Interestingly, cyclic R<sup>1</sup> substituents such as cyclopropyl 17 and cyclohexyl 18 had significantly lower potencies, indicating a strong conformational preference. These results pointed to the 3-pentyl group as the optimal substituent at this position based on its potency profile and stability in human liver microsomes.

The SAR exploration at the R<sup>2</sup> position in the context of a 3-pentyl R<sup>1</sup> group revealed specific steric and electronic preferences (Table 4). Compact, electron-rich lipophilic groups were generally preferred in this position, as exemplified by the potency loss observed when bromine (14) or chloro (21) substituent was replaced with a trifluoromethyl (22) or cyano (27) group. Vinyl analogue 24 was among the more potent compounds, but the strongest preference was for an ethynyl group (25, CK-2017357), which was 3-fold more potent than bromo 14. Notably, propynyl analogue 26 was much less active,

Table 4. Assessment of R<sub>2</sub>, N-1 Methylbenzyl Analogues

#	R <sup>2</sup>	AC <sub>40</sub> (μM)	DF <sub>30</sub> (μM)	Re (r)	Re (h)
19	H	14.0	NT	NT	NT
20	Me	2.0	4.4	0.7	<0.2
21	Cl	0.5	0.6	0.4	<0.2
14	Br	0.3	0.4	0.4	<0.2
22	CF <sub>3</sub>	11.3	NT	0.2	<0.2
23	OMe	2.2	NT	>0.7	<0.2
24	CH=CH <sub>2</sub>	1.1	1.1	>0.7	0.5
25	C≡CH	0.1	0.3	0.3	<0.2
26	C≡CCH <sub>3</sub>	>49	NT	NT	NT
27	CN	36.3	NT	<0.2	<0.2

again indicating a steric limitation in that part of the binding pocket. The microsomal stability of 14, 21, and 25 was roughly equivalent, with 25 displaying the most promising combination of potency and metabolic stability.

The importance of the hydrogen bond donor/acceptor region of 25 to biochemical potency is highlighted in Figure 2.

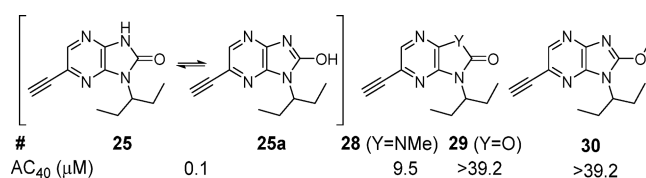
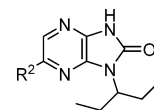


Figure 2. SAR assessment of the donor/acceptor region of 25.

Compound 25 may exist as a mixture of tautomers in solution with 25a.<sup>18</sup> Removal of the H-bond donor by either isosteric replacement of nitrogen with oxygen (29) or methylation at nitrogen (28) or oxygen (30) led to a dramatic reduction in potency.

The rat pharmacokinetic profiles for compounds with optimal potency and microsomal stability were assessed to determine their suitability for *in situ* live fiber experiments (Table 5). In rats,

Table 5. Summary Rat Pharmacokinetic Results for 14, 21, and 25



#	R <sup>2</sup>	CL (mL/min/kg)	V <sub>ss</sub> (L/kg)	F (%)	F <sub>u</sub> (r, h) <sup>a</sup> (%)
14	Br	19.0	6.5	62	1.3, 0.5
21	Cl	7.7	3.4	100	1.1, 0.8
25	C≡CH	2.6	2.6	98	6.9, 1.9

<sup>a</sup>Fu(r) or Fu(h): fraction unbound in rat (r) or human (h) plasma.

analogues 14, 21, and 25 all showed low to moderate clearance values and good oral bioavailability when dosed as crystalline suspensions. The free fraction (F<sub>u</sub>) for 25 in both human and rat plasma was greater than those for 14 and 21. Based on superior activity and oral free exposure, 25 was selected for advanced *in vivo* testing.

The sensitization of fast skeletal muscle to calcium in the presence of **25** was demonstrated using an *in situ* preparation of the extensor digitorum longus (EDL) muscle in a rat model where the nerve and the blood supply are intact.<sup>19</sup> Systemic infusion of **25** resulted in rapid, dose-dependent increases in muscle force at submaximal stimulation rates (Figure 3) without

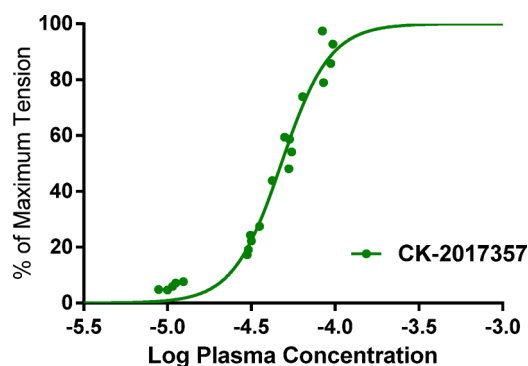


Figure 3. Rat *in situ* EDL muscle plasma concentration–force response curve with **25** (CK-20171357).

increasing the maximum tension at tetanic stimulation rates. This result was consistent with the effects of **25** on the force–calcium relationship of skinned rabbit psoas muscle fibers and the increase in ATPase rate (a surrogate for force production) in the biochemical assay.

To support pharmacology and safety studies as well as human PK and dose projections, a pharmacokinetic assessment of **25** was performed (Table 6). In a Caco-2 cell monolayer system, **25**

Table 6. *In Vitro* and *In Vivo* Pharmacokinetics of **25**

species	Re <sup>a</sup>	CL (mL/min/kg)	V <sub>ss</sub> (L/kg)	F (%)
human	<0.21			
dog	<0.21	4.3	1.7	93
rat	0.26	2.6	0.8	98
mouse	0.24	13.9	1.0	43

<sup>a</sup>Re = ratio of extraction in microsomes; PK dose = 1 mg/kg.

demonstrated high permeability (permeability coefficient of  $>50 \times 10^{-6}$  cm/s) and no apparent efflux. It showed low to moderate liver microsomal stability and relatively low *in vivo* clearance across species with values less than 15% of hepatic blood flow. Following oral administration, **25** was well absorbed with oral bioavailability ranging from 43% in mice to greater than 90% in rats and dogs. The low clearance and high bioavailability of **25** observed in nonclinical species are consistent with the high exposure following oral administration of the clinical dose in humans.<sup>20</sup>

Compound **25** exhibited moderate inhibition and time-dependent inhibition of CYP1A2 (IC<sub>50</sub> = 20 μM, IC<sub>50</sub> shift of >3 following a 30 min preincubation).<sup>21</sup> In clinical studies involving ALS patients taking both **25** and Riluzole, a drug–drug interaction (DDI) occurred that resulted in an approximate doubling of Riluzole concentrations.<sup>22</sup> Riluzole is a commonly prescribed drug for ALS that is cleared mainly by CYP1A2 and CYP1A1 mediated metabolism.<sup>23</sup> This DDI was managed in the clinic by reducing the dose of Riluzole from 100 mg/day b.i.d. to 50 mg/day q.d.

The effect of compound **25** (tiraseptiv) on muscle performance has been evaluated in preclinical and clinical models. In a

mouse model of ALS with functional deficits (B6SJL-SOD1<sup>G93A</sup>), a single dose of tiraseptiv significantly increased submaximal isometric force, forelimb grip strength, grid hang time, and rotarod performance.<sup>24</sup> Tiraseptiv also increased grip strength in rats treated with the anti-nAChRα antibody in the PT-EAMG (passive transfer experimental autoimmune myasthenia gravis) rat model.<sup>10</sup> In a clinical study performed in healthy humans, tiraseptiv increased force produced by the tibialis anterior in a dose-, concentration-, and frequency-dependent manner with the largest increases produced at subtetanic nerve stimulation frequencies.<sup>25</sup> This effect was similar to what was observed in rat EDL studies.

In conclusion, HTS hit imidazopyrazinone **1** was identified using a fast skeletal ATPase assay and demonstrated improved calcium sensitivity and force production in muscle fibers. To enable *in vivo* pharmacological testing, **1** was optimized for biochemical potency and oral exposure, leading to compound **25** (tiraseptiv). Upon intravenous administration in preclinical models, tiraseptiv showed a concentration-dependent improvement in muscle force production *in situ*. In a Phase 3 clinical trial (VITALITY-ALS, NCT02496767) in patients with ALS, tiraseptiv did not meet its primary end point, change from baseline in slow vital capacity (SVC) at 24 weeks, or any of the secondary end points. Though not reaching statistical significance, the decline in SVC was smaller in patients who received any dose of tiraseptiv compared to patients receiving placebo. The largest differences from placebo were observed in patients randomized to the mid- and high-dose groups of tiraseptiv who could tolerate and remain on their target dose, suggestive of pharmacologic activity for the mechanism of action in ALS. More patients discontinued double-blind treatment on tiraseptiv than on placebo primarily due to nonserious adverse events related to tolerability, potentially confounding the assessment of its efficacy. The limitations of tiraseptiv may be addressed with CK-2127107, the next-generation fast skeletal muscle troponin activator currently being assessed in several midstage clinical trials.<sup>26</sup>

## ■ ASSOCIATED CONTENT

### § Supporting Information

The Supporting Information is available free of charge on the ACS Publications website at DOI: 10.1021/acsmchemlett.7b00546.

Experimental procedures and analytical data(PDF)

## ■ AUTHOR INFORMATION

### Corresponding Author

\*Tel: 650-624-3229. Fax: 650-624-3010. E-mail: scollibee@cytokinetics.com.

### ORCID

Scott E. Collibee: 0000-0003-3513-4060

### Present Addresses

<sup>†</sup>(A.C.H.) GlaxoSmithKline, 709 Swedeland Road, King of Prussia, Pennsylvania 19406, United States.

<sup>‡</sup>(A.J.R.) Edgewise Therapeutics, 3415 Colorado Avenue, Boulder, Colorado 80303, United States.

<sup>§</sup>(D.J.M.) 700 Saginaw Drive, Suite 150, Redwood City, California 94063, United States.

<sup>||</sup>(W.F.B., IV) Cornell University Medical Center, 525 E 68th Street # STAR8, New York, New York 10065, United States.

<sup>⊥</sup>(M.T.) BMS, 521 Cottonwood Dr, Milpitas, California 95035, United States.

## Notes

The authors declare no competing financial interest.

## ACKNOWLEDGMENTS

We thank all members of the much larger Skeletal Muscle Program Team at CytoKinetics for their contributions.

## DEDICATION

This paper is dedicated to the memory of Alex R. Muci, a significant contributor to this research effort.

## ABBREVIATIONS

HTS, high-throughput screening; ALS, amyotrophic lateral sclerosis; TnC, troponin C; ATP, adenosine triphosphate; ATPase, enzymatic hydrolysis of adenosine triphosphate; FSK, fast skeletal muscle; CV, cardiovascular muscle; SSK, slow skeletal muscle; LE, ligand efficiency; LipE, lipophilic efficiency; SAR, structure–activity relationship; CYP, cytochrome P450 enzyme; EDL, extensor digitorum longus muscle; AC<sub>40</sub>, concentration that increases native ATPase function by 40%; DF<sub>30</sub>, concentration that increases muscle fiber tension by 30%; Re(r) and Re(h), microsomal extraction ratio in rat (r) or human (h) microsomes; F<sub>b</sub>, fraction bound in plasma; PK, pharmacokinetics; DDI, drug–drug interaction; SVC, slow vital capacity

## REFERENCES

- (1) Rowland, L. P.; Schneider, N. A. Amyotrophic lateral sclerosis. *N. Engl. J. Med.* **2001**, *344*, 1688–1700.
- (2) Kolb, S. J.; Kissel, J. T. Spinal muscular atrophy: a timely review. *Arch. Neurol.* **2011**, *68*, 979–984.
- (3) Patzkó, A.; Shy, M. E. Update on Charcot-Marie-Tooth disease. *Curr. Neurol. Neurosci. Rep.* **2011**, *11*, 78–88.
- (4) Research Group in Neuromuscular Diseases.. Classification of the neuromuscular disorders. *Lancet* **1968**, *291*, 1020–1021.
- (5) Rosenfeld, J.; Strong, M. J. Challenges in the understanding and treatment of amyotrophic lateral sclerosis/motor neuron disease. *Neurotherapeutics* **2015**, *12* (2), 317–325.
- (6) Faravelli, I.; Nizzardo, M.; Comi, G. P.; Corti, S. Spinal muscular atrophy: recent therapeutic advances for an old challenge. *Nat. Rev. Neurol.* **2015**, *11* (6), 351–359.
- (7) Baets, J.; De Jonghe, P.; Timmerman, V. Recent advances in Charcot-Marie-Tooth disease. *Curr. Opin. Neurol.* **2014**, *27* (5), 532–540.
- (8) (a) Malik, F. I.; Hartman, J. J.; Elias, K. A.; Morgan, B. P.; Rodriguez, H.; Brejc, K.; Anderson, R. L.; Sueoka, S. H.; Lee, K. H.; Finer, J. T.; Sakowicz, R.; Baliga, R.; Cox, D. R.; Garard, M.; Godinez, G.; Kawas, R.; Kraynack, E.; Lenzi, D.; Lu, P.; Muci, A.; Niu, C.; Qian, X.; Pierce, D. W.; Pokrovskii, M.; Suehiro, I.; Sylvester, S.; Tochimoto, T.; Valdez, C.; Wang, W.; Katori, T.; Kass, D. A.; Shen, Y.; Vatner, S. F.; Morgans, D. J. Cardiac myosin activation: a potential therapeutic approach for systolic heart failure. *Science* **2011**, *331*, 1439–1443.
- (9) Morgan, B. P.; Muci, A.; Lu, P.; Qian, X.; Tochimoto, T.; Smith, W. W.; Garard, M.; Kraynack, E.; Collibee, S.; Suehiro, I.; Tomasi, A.; Valdez, S. C.; Wang, W.; Jiang, H.; Hartman, J.; Rodriguez, H. M.; Kawas, R.; Sylvester, S.; Elias, K. A.; Godinez, G.; Lee, K.; Anderson, R.; Sueoka, S.; Xu, D.; Wang, Z.; Djordjevic, N.; Malik, F. I.; Morgans, D. J., Jr. Discovery of *omecamtiv mecarbil* the first, selective, small molecule activator of cardiac myosin. *ACS Med. Chem. Lett.* **2010**, *1*, 472–477.
- (10) Additional information for the mix and match experiments for **1** is included in the [Supporting Information](#). Russell, A. J.; Hartman, J. J.; Hinken, A. C.; Muci, A. R.; Kawas, R.; Driscoll, L.; Godinez, G.; Lee, K. H.; Marquez, D.; Browne, W. F., IV; Chen, M. M.; Clarke, D.; Collibee, S. E.; Garard, M.; Hansen, R.; Jia, Z.; Lu, P. P.; Rodriguez, H.; Saikali, K. G.; Schaletzky, J.; Vijayakumar, V.; Albertus, D. L.; Claffin, D. R.; Morgans, D. J.; Morgan, B. P.; Malik, F. I. Activation of fast skeletal muscle troponin as a potential therapeutic approach for treating neuromuscular diseases. *Nat. Med.* **2012**, *18*, 452–456.
- (11) Gomes, A. V.; Potter, J. D.; Szczesna-Cordary, D. The Role of Troponins in Muscle Contraction. *IUBMB Life* **2002**, *54*, 323–333.
- (12) Finer, J. T.; Malik, F.; Sakowicz, R.; Shumate, C.; Wood, K. Compositions and assays utilizing ADP or phosphate for detecting protein modulators. US 6,410,254 B1, January 18, 2007. See [Supporting Information](#) and references therein for detailed procedures for muscle protein preparation and assay methods. In general, the standard deviations of the AC<sub>40</sub> results for duplicate experiments with the ATPase assay were relatively low. Rabbit fast skeletal muscle was used in the biochemical and skinned fiber assays because of the high degree of structural similarity to human muscle, widespread use in muscle biology, and ready availability.
- (13) LE: Hopkins, A. L.; Groom, C. R.; Alex, A. Ligand efficiency: a useful metric for lead selection. *Drug Discovery Today* **2004**, *9* (10), 430–431.
- (14) LipE: Perola, E. An analysis of the binding efficiencies of drugs and their leads in successful drug discovery programs. *J. Med. Chem.* **2010**, *53* (7), 2986–2997.
- (15) Claffin, D. R.; Larkin, L. M.; Cederna, P. S.; Horowitz, J. F.; Alexander, N. B.; Cole, N. M.; Galecki, A. T.; Nyquist, L. V.; Carlson, B. M.; Faulkner, J. A.; Ashton-Miller, J. A. Effects of high- and low-velocity resistance training on the contractile properties of skeletal muscle fibers from young and older humans. *J. Appl. Physiol.* **2011**, *111*, 1021–1030.
- (16) See [Supporting Information](#) for specific syntheses of the various analogues.
- (17) Obach, R. S. Prediction of human clearance of twenty-nine drugs from hepatic microsomal intrinsic clearance data: an examination of in vitro half-life approach and nonspecific binding to microsomes. *Drug Metab. Dispos.* **1999**, *27* (11), 1350–1359.
- (18) Internal <sup>1</sup>H and <sup>13</sup>C spectroscopic data suggest that the keto tautomer **25** predominates in DMSO, methanol, and benzene. The population of keto tautomer **25** was calculated to be >99% at a pH of 7 using the EHT derived descriptor-based protomer prediction tool within MOE 2016.
- (19) Brooks, S. V.; Faulkner, J. A. Contraction-induced injury: recovery of skeletal muscles in young and old mice. *Am. J. Physiol. – Cell Physiol* **1990**, *258*, C436–C442.
- (20) Shefner, J.; Cedarbaum, J. M.; Jesse, M.; Cudkowicz, M. E.; Maragakis, N.; Lee, J.; Jones, D.; Watson, M. L.; Mahoney, K.; Chen, M.; Saikali, K.; Mao, J.; Russell, A. Safety, tolerability and pharmacodynamics of a skeletal muscle activator in amyotrophic lateral sclerosis. *Amyotrophic Lateral Scler.* **2012**, *13* (5), 430–438.
- (21) Ortiz de Montellano, P. R.; Komives, E. A. Branchpoint for Heme Alkylation and Metabolite Formation in the Oxidation of Arylacetylenes by Cytochrome P-450. *J. Biol. Chem.* **1985**, *260* (6), 3330–3336.
- (22) Shefner, J. M.; Watson, M. L.; Meng, L.; Wolff, A. A. A study to evaluate safety and tolerability of repeated doses of *tirasemtiv* in patients with amyotrophic lateral sclerosis. *Amyotrophic Lateral Scler. Frontotemporal Degener.* **2013**, *14* (7–8), 574–581.
- (23) Ajroud-Driss, S.; Saeed, M.; Khan, H.; Siddique, N.; Hung, W. Y.; Sufit, R.; Heller, S.; Armstrong, J.; Casey, P.; Siddique, T.; Lukas, T. J. Riluzole metabolism and CYP1A1/2 polymorphisms in patients with ALS. *Amyotrophic Lateral Scler.* **2007**, *8* (5), 305–309.
- (24) Hwee, D. T.; Kennedy, A.; Ryans, J.; Russell, A. J.; Jia, Z.; Hinken, A. C.; Morgans, D. J.; Malik, F. I.; Jasper, J. R. Fast Skeletal Muscle Troponin Activator *Tirasemtiv* Increases Muscle Function and Performance in the B6SJL-SOD1G93A ALS Mouse Model. *PLoS ONE.* **2014**, *9* (5), e96921.
- (25) Hansen, R.; Saikali, K. G.; Chou, W.; Russell, A. J.; Chen, M. M.; Vijayakumar, V.; Stoltz, R. R.; Baudry, S.; Enoka, R. M.; Morgans, D. J.; Wolff, A. A.; Malik, F. I. *Tirasemtiv* amplifies skeletal muscle response to nerve activation in humans. *Muscle Nerve* **2014**, *50* (6), 925–931.
- (26) Andrews, J. A.; Miller, T. M.; Vijayakumar, V.; Stoltz, R.; James, J. K.; Meng, L.; Wolff, A. A.; Malik, F. I. CK-2127107 amplifies skeletal muscle response to nerve activation in humans. *Muscle Nerve* **2017**, 26017.